Journal of Interdisciplinary Mathematics
ISSN: 0972-0502 (Print), ISSN: 2169-012X (Online)
Vol. 29 (2026), No. 6, pp. 2049–2065
DOI : 10.47974/JIM-2583

Surface waves in hygro-thermoelastic half-space with hydrostatic initial stress, rotation & magnetic field

Sumit Kumar *
Harish Nagar †
Sangeeta Kumari §
Department of Mathematics
Chandigarh University
Gharuan
Mohali 140413
Punjab
India

Abstract

This research investigates how surface waves propagate within a hygro-thermoelastic medium under the influenced by rotation, magnetic field and hydrostatic initial stress. The wave equations, which are coupled are solved which involve displacement, moisture concentration and temperature and obtain the penetration depth of different waves against frequency through graphical analysis. In this, the deformation of the medium is analyzed when a mechanical force is applied along the free surface of a hygro-thermoelastic solid, considering rotation, magnetic field and hydrostatic initial stress effects. The displacement components, moisture concentration, mechanical stresses, and temperature distribution within the medium are evaluated and graphically illustrated to demonstrate the impact of rotation, hydrostatic initial stress, and magnetic field. Overall, the research article presents analytical solutions and graphical representations of surface wave propagation and the resulting deformation in the hygro-thermoelastic medium. The impact of rotation, initial stress, and the magnetic field on various physical quantities are discussed and providing valuable insights into the behavior of the system.

Subject Classification: *74F05, 74J20, 74G60, 74B05.*

Keywords: *Hygro-thermoelastic, Rotation, Hydrostatic initial stress, Magnetic field, Surface waves, Moisture concentration, Penetration depth.*

* *E-mail:* **sumitkochar76@gmail.com (Corresponding Author)**
† *E-mail:* **drharishngr@gmail.com**
§ *E-mail:* **Sangwan.sangeeta.ss@gmail.com**

1. Introduction

Diffusion pertains to the movement of atoms as well as particles from one place to another. In a solid state, particles stay in a fixed position until they reach steady state. However, when these are disturbed, they have a tendency to move toward areas with lower concentration of themselves coming from those with higher concentration. This is aided by imperfections in the material's structure and inner stresses. With significant increase in temperature, the distance between the atoms widens leading to possible melting of the solid. Similarly, uneven distribution of wetness creates a gradient of concentrations which results in transfer of moisture. Both heat and moisture levels change with time and space inside any given substance thereby making heat transfer theories virtually interchangeable with those for moisture also. Moreover, mechanical tensions can greatly modify how temperatures or even moistures are spread out.

Moisture and temperature have combined effects on materials typical of polymers, porous composites, asphalt concrete, and geo-materials among others. Several scholars have tried to come up with models that would show how polymers and their composites behave under these conditions. For example, Sih, Shih, and Chou [1], Sih, Michopoulos, and Chou [2] conducted a numerical study on hygrothermal stresses in composites with the coupled theory of heat and moisture using experimental results. To study transient responses of structures (including infinitely long hollow cylinders and solid cylinders), Chang, Chen, and Weng [3], Chang [4] applied the linear theory of heat and moisture under hygrothermal loading. Composite materials, which are preferred due to their mechanical properties and flexibility in design, find wide application as construction elements where performance is significantly affected by hydrothermal environment. The theory for free vibration and transient's responses of multiple delaminated doubly curved composite shells under hygrothermal conditions was developed by Parhi, Bhattacharyya, and Sinha [5].

Jin and Yao [6] proposed an improved global-local model to investigate the hygrothermal behavior of utilizing thick cross-ply laminated composite plates. Lee et al. [7] employed the classical laminated plate theory combined with Von Karman's large deflection theory, investigated the cylindrical bending behavior of angle-ply plates subjected to uniformly distributed transverse loading under various support conditions by considering hygrothermal effects. Meanwhile, Shen [8] employed a micro-to-macro mechanical analytical approach to look into how hygrothermal states affect shear deformable cylindrical panels' buckling and post-buckling performance subjected to axial compression. Because of various layers have different coefficients of thermal expansions and wet expansion coefficient among materials so complex internal stresses or strains will be induced within composites when exposed in humid/hot environments leading to remarkable changes in their physical and mechanical properties after moisture absorption, the analysis of elastic problems under hygrothermal conditions is of significant importance. In their study, Gasch, Malm, and Ansell [9] formulated a coupled hygro-thermo-mechanical framework for hardened concrete; they utilized the micro-prestress solidification theory. A coupled hygro-thermo-mechanical damage model for concrete at elevated temperatures was proposed by Li and Liu [10], Gawin and Pesavento [11] formulated a mathematical approach to examine the hygrothermal response of concrete exposed to elevated temperatures. This model treats concrete as a multiphase porous medium while considering material degradation. Moreover, Beneš and Stefan [12] came up with a mathematical model that makes it possible to study mechanical and hygrothermal effects concurrently leading to spalling in concrete walls when they are exposed to high temperatures. Such environmental conditions present bigger challenges to different structures than usual mechanical loads do thus emphasizing the importance of investigating isotropic hygro-thermoelastic materials. A mathematical framework for investigating coupled hygro-thermo-mechanical spalling in concrete walls at elevated temperatures was introduced by Beneš and Stefan [12]. These effects challenge many structures more than the conventional mechanical loads do, which emphasizes the importance of investigating isotropic hygro-thermoelastic materials. On an experimental way, Benkhedda, Tounsi, and Addabedia [13] established an approximate model to evaluate the hygro-thermoelastic stresses in laminated composite plates. They were evaluating the desorption phase stresses without considering the moisture concentration specifically.

An experiment was carried out by Zenkour [14] which involved analyzing the deformation behavior of a functionally graded plate supported on an elastic base in hygrothermal environment. Similarly, Zenkour [15] derived a solution for the hygrothermal responses of non-homogeneous piezoelectric hollow cylinders subjected to mechanical and electrical loading. The authors Chiba and Sugano [16] studied moisture and transient heat transfer processes to derive the stress field arising from these conditions in layered plates subjecting one dimensional unsteady-state diffusion as unidirectional coupled problem while ignoring heat transfer effects induced by moisture content. The hygrothermal field within porous media has been investigated by Ishihara, Ootao, and Kameo [17] taking into account nonlinear coupling between moisture and heat.

A coupled piezoelectric finite element formulation considering hygrothermal strain effects was proposed by Raja et al. [18] using the virtual work approach and a nine-noded field-consistent Lagrangian element. A micromechanical approach for analyzing the response of multiphase composites was developed by Aboudi and Williams [19]. The effects of thermal and moisture conditions on the free vibration and transient response of multidirectional composites were analyzed by Rao and Sinha [20]. Zhao et al. [21] presented a steady-state general solution for three-dimensional hygro-thermoelastic media based on potential theory. Tong et al. [22] have found five 2D steady-state general solutions for isotropic hygro-thermoelastic media. The initial stress parameter is used in many fields including engineering structures, geophysics, biological tissues among others as it helps to evaluate different materials mechanical responses.

Initial stress effects in isotropic thermoelasticity were considered by Montanaro [23], and the work was later investigated and implemented by

Othman and Song [24], Singh, Kumar, and Singh [25], and Singh [26, 27]. Abo-Dahab [28] looked at the amplitude attenuation and speed of Rayleigh waves. He also examined reflection coefficients under different influences such as initial stress and magnetic fields. The propagation of plane waves in anisotropic fiber-reinforced media was analyzed by Abbas and Othman [29], while Othman and Atwa [30] explored the governing equations of generalized thermoelasticity for isotropic media with initial stress. The reflection of plane waves in a micropolar orthotropic magneto-thermoelastic half-space under impedance boundary conditions and nonlocal elasticity was investigated by Yadav et al. [31]. The use of fractional order calculus is widely used in porous and biological materials which as moisture diffusion often deviates from classical Fick's law with help of fractional order calculus diffusion equations models accurately. Kapila, Nagar, and Sharma [32] defined broader scope of fractional integration and differentiation by incorporating the Modified Bessel function with the MSM operator.

Ailawalia, Gupta, and Sharma [35] reviewed the surface waves propagation in a hygro-thermoelastic medium in the presence of hydrostatic initial stress and obtained analytical solution for displacement, stresses, thermal, and moisture content, illustrating the influence of hydrostatic initial stress through graphical results. Zhao et al. [36] developed the generalized steady-state solution for three-dimensional hygro-thermoelastic medium using the method of potential theory and applied it to boundary value problems involving moisture and thermal effects. Kumar, Nagar, and Kumari [37, 41] evaluated propagation of wave in hygro-thermoelastic media, including the reflection of plane waves at an interface and the behavior of coupled longitudinal and transverse waves in a micropolar hygro-thermoelastic medium. Ailawalia et al. [38] investigated two-dimensional distortion in a non-homogeneous hygro-thermoelastic layer with hydrostatic initial stress and obtained analytical expressions for displacement, stresses, temperature, and moisture concentration using the normal mode technique. Kumari, Bharti, and Singh [39] studied surface wave propagation in a two-temperature generalized magneto-thermoelastic medium with hydrostatic initial stress and derived the frequency equation of Rayleigh waves, illustrating the effects of different parameters through numerical results. Rayleigh wave propagation in a generalized thermoelastic half-space subjected to magnetic field, rotational effects, initial stress, and two-temperature parameter was investigated by Sharma and Kumari [40], with velocity and attenuation behaviors illustrated graphically.

2. Basic Equations

(i) The stress tensor equation defined as,

$$\sigma_{ij,j} = \rho[(2\Omega + \dot{u})_{,i} + \ddot{u}(\Omega \times \Omega \times u)_i] - \bar{\sigma}_{ji,i}, \tag{1}$$

(ii) The heat conduction equation as,

$$D_T^m m_{,ii} + D_T T_{ii} - \frac{\beta_{ij}^T T_0}{\rho c}\, \dot{u}_{j,j} - \dot{T} = 0, \tag{2}$$

(iii) Coupled moisture diffusion equation is given as

$$D_m m_{,ii} + D_m^T T_{,ii} - \dot{m} - \frac{\beta_{ij}^m m_0 D_m}{k_m} \dot{u_{J,J}} = 0, \tag{3}$$

where,

$$\beta_{ij}^T = \beta_T \delta_{ij}, \beta_T = \alpha_T(3\lambda + 2\mu), \tag{4}$$

$$\beta_{ij}^m = \beta_m \delta_{ij}, \beta_m = \alpha_m(3\lambda + 2\mu), \tag{5}$$

$$\sigma_{ij} = -P\left(\delta_{ij} + \bar{\omega}_{ij}\right) + C_{ijkl}\, \epsilon_{kl} - \beta_{ij}^m m - \beta_{ij}^T T, \tag{6}$$

$$c_{ijkl} = \frac{2G\nu}{1-2\nu}\delta_{ij}\delta_{kl} + G\delta_{ik}\delta_{ji} + G\delta_{il}\delta_{jk}, \tag{7}$$

$$\epsilon_{ij} = \frac{u_{j,i}+u_{i,j}}{2}, \bar{\omega}_{ij} = \frac{u_{j,i}-u_{i,j}}{2}, \tag{8}$$

$$\Delta \times E = -\mu_e \frac{\partial h}{\partial t}, \Delta \times h = j, \Delta \cdot h = 0, \Delta \cdot E = 0, \tag{9}$$

$$\bar{\sigma}_{ij} = \mu_e\left[H_j h_i + H_i h_j - (H.h)\delta_{ij}\right], \tag{10}$$

Where $H = H_0 + h$ and $h = \nabla \times (\mu \times H_0)$

H denotes the disturbed magnetic field superimposed on the initial field H_0, j denotes the density of electric current, where the parameter μ_e signifies magnetic permeability.

3. Problem Formulation

Let us consider 3D cartesian coordinate system, in which z-axis taken in vertically downward direction. Assuming that wave propagation takes place in the x-z plane, the hygro-thermoelastic medium is expressed in the form of displacement vector as $\vec{u} = (u, 0, w)$, with $u = u(x, z, t)$ and $w = w(x, z, t)$. Under these assumptions, the governing equations of motion, together with the generalized coupled heat and moisture transfer equations (1)-(3) and the constitutive relations eq. (6), are simplified to a two-dimensional case without body forces given below.

$$(2\mu + \lambda + H_0^2\mu_e)\frac{\partial^2 u}{\partial x^2} + \left(2\mu + \lambda + \frac{P}{2} + H_0^2\mu_e\right)\frac{\partial^2 w}{\partial x \partial z} + \left(\mu - \frac{P}{2}\right)\frac{\partial^2 u}{\partial z^2} - \beta_m \frac{\partial m}{\partial x} - \beta_T \frac{\partial T}{\partial x} = \rho(\ddot{u} - \Omega^2 u + 2\Omega\dot{w}) \tag{11}$$

$$(2\mu + \lambda + H_0^2\mu_e)\frac{\partial^2 w}{\partial z^2} + \left(2\mu + \lambda + \frac{P}{2} + H_0^2\mu_e\right)\frac{\partial^2 u}{\partial x \partial z} + \left(\mu - \frac{P}{2}\right)\frac{\partial^2 w}{\partial z^2} - \beta_m \frac{\partial m}{\partial z} - \beta_T \frac{\partial T}{\partial z} = \rho(\ddot{w} - \Omega^2 w + 2\Omega\dot{u}) \tag{12}$$

$$D_T\Delta^2 T - D_T^m \Delta^2 m - \frac{\partial T}{\partial t} - \frac{\beta_T T_0}{\rho c}\frac{\partial}{\partial t}\left(\frac{\partial u}{\partial x} + \frac{\partial w}{\partial z}\right) = 0 \tag{13}$$

$$D_m\Delta^2 m - D_m^T \Delta^2 T - \frac{\partial m}{\partial t} - \frac{\beta_m m_0 D_m}{k_m}\frac{\partial}{\partial t}\left(\frac{\partial u}{\partial x} + \frac{\partial w}{\partial z}\right) = 0 \tag{14}$$

$$\sigma_{xx} = -P + \lambda\frac{\partial w}{\partial z} + (\lambda + 2\mu)\frac{\partial u}{\partial x} - \beta_m m - \beta_T T \tag{15}$$

$$\sigma_{xz} = \left(\mu + \frac{P}{2}\right)\frac{\partial u}{\partial z} + \left(\mu - \frac{P}{2}\right)\frac{\partial w}{\partial x} \quad (16)$$

$$\sigma_{zx} = \left(\mu - \frac{P}{2}\right)\frac{\partial u}{\partial z} + \left(\mu + \frac{P}{2}\right)\frac{\partial w}{\partial x} \quad (17)$$

$$\sigma_{zz} = -P + \lambda\frac{\partial u}{\partial x} + (\lambda + 2\mu)\frac{\partial w}{\partial z} - \beta_m m - \beta_T T \quad (18)$$

Where, λ and μ are Lame's constant, D_m denotes Diffusion coefficient of moisture, D_T denotes temperature diffusivity, β_T, β_m denotes the coupled diffusivity, m_0 is the reference moisture, ρ denotes the density of the medium, temperature denotes by T, P denotes initial stress, and $\sigma_{ij,j}$ corresponds to the stress vector.

To facilitate numerical analysis, the following dimensionless parameters are employed:

$$x' = \frac{x}{l}, z' = \frac{z}{l}, u' = \frac{u}{l}, w' = \frac{w}{l}, t' = \frac{D_m t}{l^2}, m' = m, T' = \frac{T}{T_0}, \sigma_{ij}' = \frac{\sigma_{ij}}{\lambda}, \quad (19)$$

Here, the parameter l possesses the dimension of length.

Using eq. (19) in eq. (11)-(14)

$$(\lambda + 2\mu + \mu_e H_0^2)\frac{\partial^2 u}{\partial x^2} + \left(\lambda + 2\mu + \frac{P}{2} + \mu_e H_0^2\right)\frac{\partial^2 w}{\partial x \partial z} + \left(\mu - \frac{P}{2}\right)\frac{\partial^2 u}{\partial z^2} - \beta_m \frac{\partial m}{\partial x} - \beta_T T_0 \frac{\partial T}{\partial x} = \rho\left(\frac{D_m}{l^2}\frac{\partial^2 u}{\partial t^2} - \Omega^2 l^2 u + 2\Omega D_m \frac{\partial w}{\partial t}\right) \quad (20)$$

$$(\lambda + 2\mu + \mu_e H_0^2)\frac{\partial^2 w}{\partial z^2} + \left(\mu - \frac{P}{2}\right)\frac{\partial^2 w}{\partial x^2} + \left(\lambda + 2\mu + \frac{P}{2} + \mu_e H_0^2\right)\frac{\partial^2 u}{\partial x \partial z} - \beta_m \frac{\partial m}{\partial z} - \beta_T T_0 \frac{\partial T}{\partial z} = \rho\left(\frac{D_m}{l^2}\frac{\partial^2 w}{\partial t^2} - \Omega^2 l^2 w + 2\Omega D_m \frac{\partial u}{\partial t}\right) \quad (21)$$

$$D_T^m \Delta^2 m - D_T T_0 \Delta^2 T + D_m T_0 \frac{\partial T}{\partial t} + \frac{\beta_T T_0 D_m}{\rho c}\frac{\partial}{\partial t}\left(\frac{\partial u}{\partial x} + \frac{\partial w}{\partial z}\right) = 0 \quad (22)$$

$$D_m \Delta^2 m - D_m^T T_0 \Delta^2 T - D_m \frac{\partial m}{\partial t} - \frac{\beta_m m_0 D_m^2}{k_m}\frac{\partial}{\partial t}\left(\frac{\partial u}{\partial x} + \frac{\partial w}{\partial z}\right) = 0 \quad (23)$$

According to the "Helmholtz representation", the displacement variables u and w can be written as the potential variables q and ψ.

$$u = \frac{\partial q}{\partial x} - \frac{\partial \psi}{\partial z}, w = \frac{\partial q}{\partial x} + \frac{\partial \psi}{\partial z}, \quad (24)$$

Using eq. (24) in eq. (20) - (23), we obtain

$$(\lambda + 2\mu + \mu_e H_0^2)\left(\frac{\partial^2 q}{\partial x^2} + \frac{\partial^2 q}{\partial z^2}\right) - \beta_m m - \beta_T T_0 T = \rho\left(\frac{D_m^2}{l^2}\ddot{q} - \Omega^2 l^2 q + 2\Omega D_m \dot{\psi}\right), \quad (25)$$

$$\left(\mu - \frac{P}{2}\right)\Delta^2\psi = \rho\left(\frac{D_m^2}{l^2}\ddot{\psi} - \Omega^2 l^2 \psi + 2\Omega D_m \dot{q}\right), \quad (26)$$

$$D_T^m \Delta^2 m - D_T T_0 \Delta^2 T + D_m T_0 \frac{\partial T}{\partial x} + \frac{\beta_T T_0 D_m}{\rho c}\frac{\partial}{\partial t}(\Delta^2 q) = 0, \quad (27)$$

$$D_m \Delta^2 m + D_m^T T_0 \Delta^2 T - D_m \frac{\partial m}{\partial t} - \frac{\beta_m m_0 D_m^2}{k_m}\frac{\partial}{\partial t}(\Delta^2 q) = 0, \quad (28)$$

4. Equation of frequency along with Solution

Assuming waves propagation in x-z plane then solution of eq. (25) - (28) taken as:

$$m, \psi, T, q \ = \left(\overline{m}, \overline{\psi}, \overline{T}, \overline{q}\right) e^{i\xi(x+kz-\nu t)}, \tag{29}$$

Where the ratio $\nu = \frac{\omega}{\xi}$ gives phase velocity, k represents the wave penetration depth and ω is frequency.

Using eq. (29) in eq. (25)-(28), the equations obtained are as follows,

$$(a_{11}(1+k^2) - a_{12} + a_{13})\overline{q} - \beta_m \overline{m} - \beta_T T_0 \overline{T} + a_{14}\overline{\psi} = 0, \tag{30}$$

$$\left(a_{11} + a_{13} - a_{21}(a + k^2)\right)\overline{\psi} - (a_{14})\overline{q} = 0, \tag{31}$$

$$a_{31}(1+k^2)\overline{q} + (1+k^2)a_{32}\overline{m} + \left((1+k^2)a_{33} - a_{34}T_0\right)\overline{T} = 0, \tag{32}$$

$$(1+k^2)a_{41}\overline{q} + \left((1+k^2)a_{42} - a_{34}\right)\overline{m} + (1+k^2)a_{43}\overline{T} = 0, \tag{33}$$

Where,

$$a_{11} = \frac{\rho D_m^2 \omega^2}{l^2}, a_{12} = \lambda + 2\mu + \mu_e H_0^2, a_{13} = \Omega^2 l^2 \rho, a_{14} = 2i\rho\omega\Omega D_m,$$

$$a_{21} = \left(\mu - \frac{P}{2}\right)\xi^2, a_{31} = \frac{i\xi^2\omega\beta_T T_0 D_m}{\rho c}, a_{32} = D_T^m \xi^2, a_{33} = D_T \xi^2 T_0,$$

$$a_{34} = i\omega D_m, a_{41} = i\omega\beta_m m_0 \xi^2 k_m D_m^2, a_{42} = \xi^2 D_m, a_{43} = \xi^2 D_m^T T_0 .$$

After obtaining the solution of coupled eq. (30)-(33), we obtain eight-degree equation as follows,

$$A_1 k^8 + A_2 k^6 + A_3 k^4 + A_4 k^2 + A_5 = 0 \,. \tag{34}$$

Where,

$A_1 = \eta_1$,

$A_2 = 4\eta_1 + \eta_2$,

$A_3 = 6\eta_1 + 3\eta_2 + \eta_3$,

$A_4 = 4\eta_1 + 3\eta_2 + 2\eta_3 + \eta_4$,

$A_5 = \eta_1 + \eta_2 + \eta_3 + \eta_4 + \eta_5$,

$$\eta_1 = a_{11}a_{21}a_{33}a_{42},$$

$$\begin{aligned}\eta_2 = &-a_{11}^2 a_{33}a_{42} - a_{11}a_{13}a_{33}a_{42} - a_{11}a_{21}a_{32}a_{43} - a_{11}a_{21}a_{34}a_{42}T_0 \\ &-a_{11}a_{21}a_{33}a_{34} - a_{12}a_{21}a_{33}a_{42} + a_{13}a_{21}a_{33}a_{42} - a_{21}a_{32}a_{41}\beta_T T_0 \\ &+a_{21}a_{31}\beta_T T_0 + a_{21}a_{33}a_{41}\beta_m ,\end{aligned}$$

$$\begin{aligned}\eta_3 = &\, a_{14}^2(a_{34} - a_{33})a_{42} + a_{11}^2 a_{32}a_{43} + a_{11}a_{13}a_{32}a_{43} + a_{11}^2 a_{34}a_{42}T_0 \\ &+a_{11}a_{13}a_{34}a_{42}T_0 + a_{11}^2 a_{34}a_{33} + a_{11}a_{13}a_{33}a_{34} + a_{11}a_{12}a_{33}a_{42} \\ &+a_{12}a_{13}a_{33}a_{42} - a_{11}a_{13}a_{33}a_{42} - a_{13}^2 a_{33}a_{42} + a_{11}a_{32}a_{41}\beta_{T_0} \\ &+a_{13}a_{32}a_{41}\beta_T T_0 - a_{11}a_{31}a_{42}\beta_T T_0 - a_{13}a_{31}a_{42}\beta_T T_0 - a_{11}a_{33}a_{41}\beta_m\end{aligned}$$

$$-a_{13}a_{33}a_{41}\beta_m + a_{11}a_{21}a_{34}a_{34}T_0 + a_{12}a_{21}a_{32}a_{43} + a_{12}a_{21}a_{34}a_{42}T_0$$
$$+a_{12}a_{21}a_{33}a_{34} + a_{13}a_{21}a_{32}a_{43} + a_{13}a_{21}a_{34}a_{42}T_0 + a_{13}a_{21}a_{33}a_{34}$$
$$-a_{21}a_{31}a_{43}\beta_m - a_{21}a_{31}a_{34}\beta_T T_0 - a_{21}a_{34}a_{41}\beta_m T_0$$
$$\eta_4 = \mathrm{T}_0(a_{13}a_{34}a_{41}\beta_m + a_{14}^2 a_{34}a_{42} - a_{11}^2 a_{34}^2 - a_{11}a_{13}a_{34}^2$$
$$-a_{11}a_{12}a_{34}a_{42} - a_{12}a_{13}a_{34}a_{42} - a_{11}a_{13}a_{34}a_{42} - a_{13}^2 a_{34}a_{42}$$
$$+a_{11}a_{31}a_{34}\beta_T + a_{13}a_{31}a_{34}\beta_T + a_{11}a_{34}a_{41}\beta_m - a_{12}a_{21}a_{34}^2$$
$$+a_{21}a_{13}a_{34}^2) - a_{14}^2 a_{32}a_{34}a_{14}^2 a_{33}a_{34} - a_{11}a_{12}a_{32}a_{43}$$
$$-a_{12}a_{13}a_{32}a_{43} - a_{11}a_{12}a_{33}a_{34} - a_{12}a_{13}a_{33}a_{34} - a_{11}a_{13}a_{32}a_{43}$$
$$-a_{13}^2 a_{32}a_{43} - a_{11}a_{13}a_{33}a_{34} - a_{13}^2 a_{33}a_{34} + a_{11}a_{31}a_{43}\beta_m$$
$$+a_{13}a_{31}a_{43}\beta_m$$
$$\eta_5 = -a_{34}^2 a_{14}^2 T_0 + a_{12}a_{34}^2 a_{11}T_0 + a_{13}a_{34}^2 a_{12}T_0 - a_{11}a_{34}^2 a_{13}T_0 - a_{34}^2 a_{13}^2 T_0$$

Subject to the radiation condition $u, w, T, m \to 0$as $z \to \infty$, the solution of Eqs. (30)–(34) is obtained in the form:

$$[q, m, T, \psi] = (\sum_{n=1}^{4} P_n, Q_n, R_n, S_n \exp\{-i\xi k_n z\})\exp\{i\xi(x - \nu t)\} \quad (35)$$

Where k_n^2 (n=1, 2, 3, 4) are the roots of the Equ. (34) and using Equ. (35), we get

$$P_n = F^* S_n \quad (36)$$
$$Q_n = F^{**} S_n \quad (37)$$
$$R_n = F^{***} S_n \quad (38)$$

5. Boundary Conditions

To evaluate unknown parameters, considering $\mathrm{S_n}$ is the boundary conditions imposed at the surface $\mathrm{z} = 0$ are expressed as follows:

$$\sigma_{zz} = -Fexp\{i\xi(x - \nu t)\}, \sigma_{zx} = 0, \frac{\partial T}{\partial z} = 0, \frac{\partial m}{\partial z} = 0. \quad (39)$$

Where (n = 1,2,3,4),

Using eq. (6), (24), (35) respectively in boundary conditions eq. (39), The governing expressions for mechanical stress and displacement components for hygro-thermoelastic medium under the influence of hydrostatic initial stress are given below:

$$u = i\xi\left(\sum_{n=1}^{4}(F^* + k_n)S_n \exp(-i\xi k_n z)\exp\left(i\xi(x - \nu t)\right)\right), \quad (40)$$
$$w = i\xi\left(\sum_{n=1}^{4}(1 - k_n F^*)S_n \exp(-i\xi k_n z)\exp\left(i\xi(x - \nu t)\right)\right), \quad (41)$$
$$\sigma_{zz} = \left(-\frac{P}{\lambda} - \xi^2(F^* + k_n) - \xi^2 k_n\left(1 + 2\frac{\mu}{\lambda}\right)(1 + F^*) - \frac{\beta_m}{\lambda}F^{**} - \frac{\beta_T T_0}{\lambda}F^{***}\right)$$
$$\exp(-i\xi k_n z)\exp\left(i\xi(x - \nu t)\right), \quad (42)$$
$$\sigma_{zx} = \left(\left(\mu - \frac{P}{2}\right)\xi^2 k_n(F^* + k_n) + \left(\mu - \frac{P}{2}\right)\xi^2(k_n F^* - 1)\right)$$
$$\exp(-i\xi k_n z)\exp\left(i\xi(x - \nu t)\right). \quad (43)$$

Making use of the solutions eq. (37) to eq. (39) in boundary conditions eq. (38), A non-zero solution is expressed as:

$$\Delta = \frac{1}{F_0}[(N_3O_4 - N_4O_3)(H_1M_2 - H_2M_1) + (N_2O_4 - O_2N_4)(H_3M_1 - H_1M_3)$$
$$+(H_1M_4 - H_4M_1)(O_3N_2 - N_3O_2) + (M_3H_2 - H_3M_2)(O_4N_1 - N_4O_1)$$
$$+(H_4M_2 - H_2M_4)(O_3N_1 - N_3O_1) + (M_4H_3 - H_4M_3)(O_2N_1 - N_2O_1)]$$

6. Numerical Result and Discussions

For validating the analytical findings presented earlier, an illustrative numerical example involving a wood slab considered as a porous medium. The required physical quantities are taken from Chang and Weng [33] and Yang et al. [34].

$\lambda = 46.92 \times 10^9 Nm^{-2}, \rho = 370\ kgm^{-3}, \nu = 0.33, m_0 = 10\%,$
$\mu = 24.17 \times 10^9 Nm^{-2}, \alpha^m = 2.68 \times 10^{-3} cm\ /cm\ (\%H_2O), T_0 = 283K,$
k = 0.65 w/m, $\alpha^T = 31.3 \times 10^{-6} cm/cm$, c = 2500J/Kg, $k_m = 2.2 \times 10^{-8} \frac{kg}{msM}$,
$D_m = 2.16 \times 10^{-6}\ m^2/sec, D_T = \frac{k}{\rho c}, D_m^T = 0.648 \times 10^{-6}\ m^2(\%H_2O)/s(K),$
$D_m^T = 0.648 \times 10^{-6}\ m^2(K)/s(\%H_2O)$

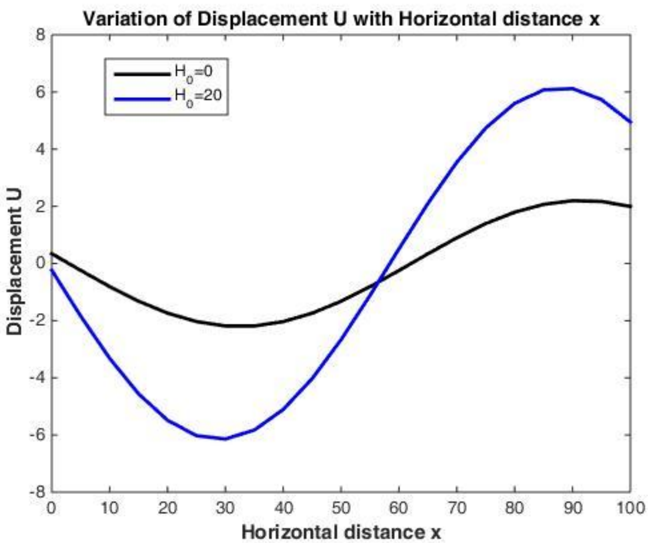

Figure 1
Variation of Displacements U along the horizontal distance x

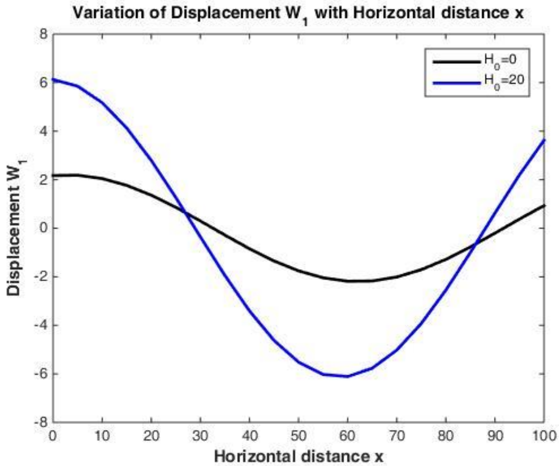

Figure 2
Variation of Displacements W_1 along the horizontal distance x

Figure 1-2 shows that the variation of displacements W_1 and U along the horizontal distance x. In Figure 1, for $H_0 = 0, \xi = 20$ the displacement initially decreases with an increase in horizontal distance then instantly increase and finally decreases again. For $H_0 = 20, \xi = 20$ the displacement initially decreases, followed by a slight increase, and subsequently decreases again. In Figure 2, for $H_0 = 0, \xi = 20$ the displacement decreases initially then slightly increases, and finally decreases. Whereas $H_0 = 20, \xi = 20$ the displacement first decrease, then instantly increases and finally decreases with increasing horizontal distance.

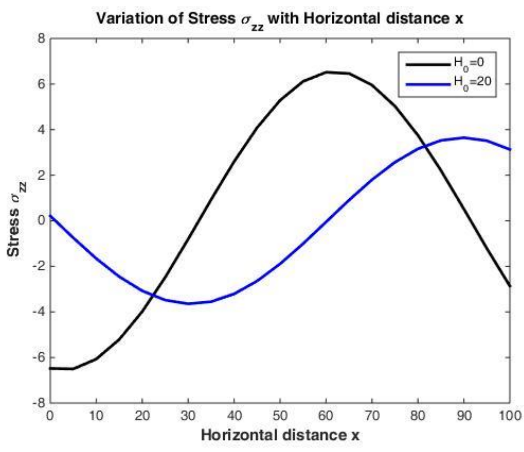

Figures 3
Variation of Stresses σ_{zz} along the horizontal distance x

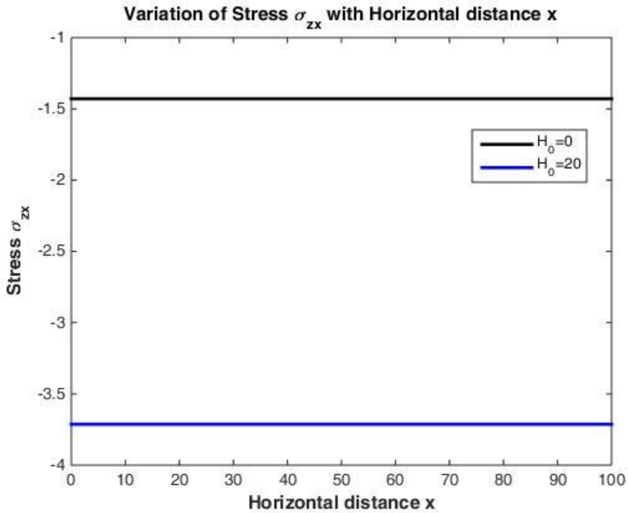

Figures 4
Variation of Stresses σ_{zx} along the horizontal distance x

Figure 3-4 shows that the variation between Stresses σ_{zz} and σ_{zx} along the horizontal distance. In Figure 3 for $H_0 = 0, \xi = 20,$ the stress initially decreases with increasing horizontal distance, then instantly increases, and finally decreases again. For $H_0 = 20, \xi = 20$ the stress first decreases, then increases, and finally decreases. In Figure 4 for $H_0 = 0, \xi = 20$ and $H_0 = 20, \xi = 20$, the stress σ_{zx} remains constant with increasing horizontal distance.

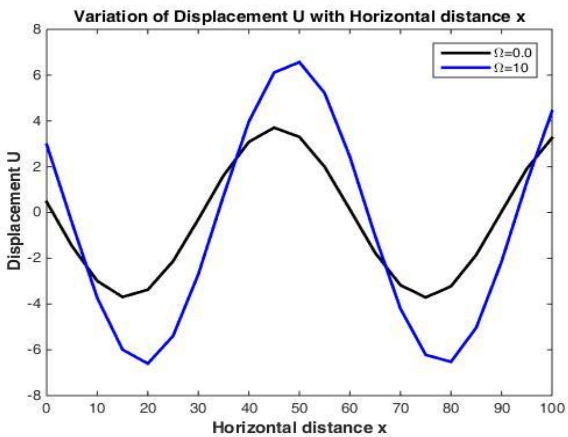

Figures 5
Variation of Displacements U along the Horizontal distance x

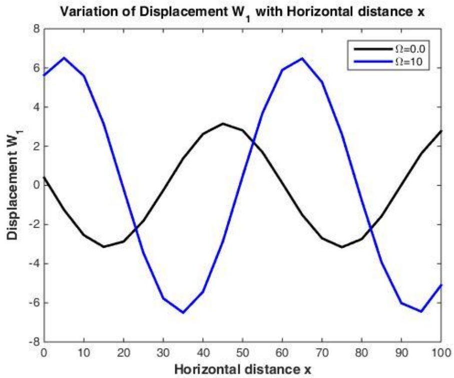

Figures 6
Variation of Displacements W_1 along the Horizontal distance x

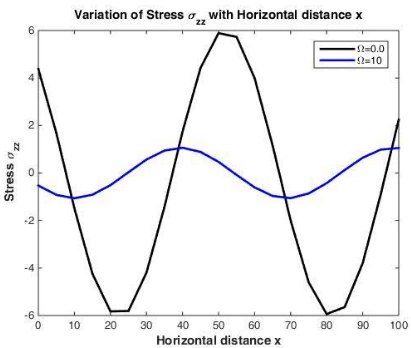

Figures 7
Variation of stress σ_{zz} along the Horizontal distance x

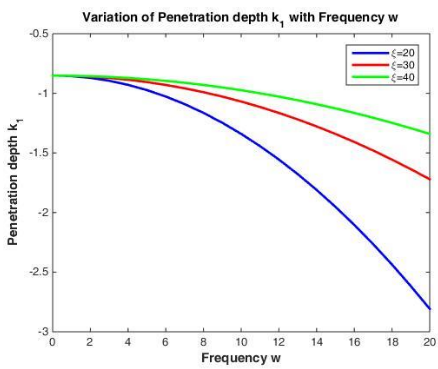

Figures 8
Penetration depth k_1 along with frequency w.

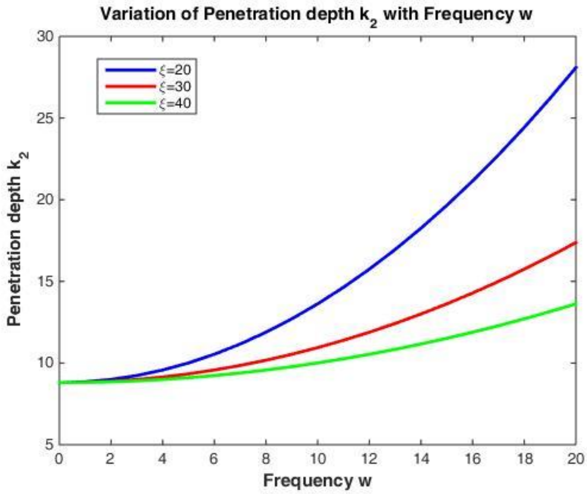

Figures 9
Penetration depth k_2 along with frequency w.

Figures 5-7 shows that the variation of displacements U, W_1 and stress σ_{zz} along the x horizontal distance for distinct values of the Ω (rotation). For $\Omega = 0, \xi = 20$, the displacement initially decreases with increasing horizontal distance, then increases, followed by another decrease and increase, while the stress σ_{zz} show sharp oscillatory behavior. For $\Omega = 10$, $\xi = 20$ both displacement and stress comparatively smoother variations, with an initial decrease followed by a slight or sharp increase and subsequent decrease. The results indicate that the rotation parameter Ω significantly influences the behavior of displacement and stress distributions.

Figures 8–9 show the variation of penetration depths $k_1$and $k_2$with frequency ω in the influence of rotation and magnetic field. Figure 8 indicates that k_1 decreases with increasing frequency ω, with a more significant decrease for smaller values of ξ, while larger values of ξ produce a smoother variation. In contrast, Figure 9 shows that k_2 increases with increasing frequency ω. The increase is steeper for smaller values of ξ, whereas higher values of ξ reduce the rate of variation.

7. Conclusion

The theory provides a realistic model for materials ranging from aerospace manufacturing, polymer manufacturing to biological tissues. The wave penetration depth and the corresponding displacement, stress, moisture, and thermal components in the medium have been analyzed, and the major findings are presented as follows:

i. The displacement wave will more sharply be decreasing when the magnetic field is present and without magnetic field the displacement wave gradually decreases than increases.

ii. When a magnetic field is present, the stress will be gradually decreasing then increasing whereas, without the presence of a magnetic field, the stress will be sharply increasing.

Likewise, different combinations of parameters have been analyzed and presented through graphical representations. The obtained results indicate a significant influence of initial hydrostatic stress, rotation and magnetic field on the displacement, moisture concentration, stress and temperature distributions.

References

[1] G. C. Sih, M. T. Shih, and S. Chou, "Transient Hygrothermal Stresses in Composites: Coupling of Moisture and Heat with Temperature Varying Diffusivity," *Int. J. Eng. Sci.,* vol. 18, no. 1, pp. 19–42 (1980).

[2] G. C. Sih, J. G. Michopoulos, and S. C. Chou, Eds., *Hygrothermoelasticity*. Dordrecht, The Netherlands: Martinus Nijhoff Publishers (1986).

[3] W. J. Chang, T. -C. Chen, and C.-I. Weng, "Transient Hygrothermal Stresses in an Infinitely Long Annular Cylinder: Coupling of Heat and Moisture," *J. Therm. Stresses*, vol. 14, no. 4, pp. 439–454 (1991).

[4] W. J. Chang, "Transient Hygrothermal Responses in a Solid Cylinder by Linear Theory of Coupled Heat and Moisture," *Appl. Math. Modell.*, vol. 18, no. 8, pp. 467–473 (1994).

[5] P. K. Parhi, S. K. Bhattacharyya, and P. K. Sinha, "Hygrothermal effects on the dynamic behavior of multiple delaminated composite plates and shells," *J. Sound Vib.*, vol. 248, no. 2, pp. 195–214 (2001).

[6] Q. Jin and W. Yao, "Hygrothermal analysis of laminated composite plates in terms of an improved C0-type global-local model," *Aerosp. Sci. Technol.,* vol. 63, pp. 328-343 (2017).

[7] S. Y. Lee, C. J. Chou, J. L. Jang, and J. S. Lin, "Hygrothermal effects on the linear and nonlinear analysis of symmetric angle-ply laminated plates," *Compos. Struct.,* vol. 21, no. 1, pp. 41–48 (1992).

[8] H. S. Shen, "Hygrothermal effects on the postbuckling of axially loaded shear deformable laminated cylindrical panels," *Compos. Struct.,* vol. 56, no. 1, pp. 73–85 (2002).

[9] T. Gasch, R. Malm, and A. Ansell, "A coupled hygro-thermo-mechanical model for concrete subjected to variable environmental conditions," *Int. J. Solids. Struct.,* vol. 91, pp. 143–156 (2016).

[10] Z. Y. Li and Y. X. Liu, "Coupled thermo-hygro-mechanical damage model for concrete subjected to high temperatures," *Appl. Math. Mech.,* vol. 33, no. 4, pp. 465–482 (2012).

[11] D. Gawin and F. B. A. Pesavento, "Modelling of hygro-thermal behaviour of concrete at high temperature with thermochemical and mechanical material degradation," *Comp. Method Appl. Mech. and Eng.,* vol. 192, no. 13–14, pp. 1731–1771 (2003).

[12] M. Beneš and R. Stefan, "Hygro-thermo-mechanical analysis of spalling in concrete walls at high temperatures as a moving boundary problem," *Int. J. Heat Mass. Trans.*, vol. 85, pp. 110–134 (2015).

[13] A. Benkhedda, A. Tounsi, and E. A. Addabedia, "Effect of Temperature and Humidity on Transient Hygrothermal Stresses During Moisture Desorption in Laminated Composite Plates," *Compos. Struct.,* vol. 82, no. 4, pp. 629–635 (2008).

[14] A. Zenkour, "Hygro-Thermo-Mechanical Effects on FGM Plates Resting on Elastic Foundations," *Compos. Struct.,* vol. 93, no. 1, pp. 234–238 (2010).

[15] A. Zenkour, "Hygrothermoelastic Responses of Inhomogeneous Piezoelectric and Exponentially Graded Cylinders," *Int. J. Pressure Vessels Piping,* vol. 119, pp. 8–18 (2014).

[16] R. Chiba and Y. Sugano, "Transient Hygrothermoelastic Analysis of Layered Plates with One-Dimensional Temperature and Moisture Variations Through the Thickness," *Compos. Struct*., vol. 93, no. 9, pp. 2260–2268 (2011).

[17] M. Ishihara, Y. Ootao, and Y. Kameo, "Hygrothermal Field Considering Nonlinear Coupling Between Heat and Binary Moisture Diffusion in Porous Media," *J. Therm. Stresses*, vol. 37, no. 10, pp. 1173–1200 (2014).

[18] S. Raja, P. K. Sinha, G. Prathap, and D. Dwarakanathan, "Influence of active stiffening on dynamic behaviour of Piezohygro-thermo-elastic composite plates and shells," *J. Sound Vib.*, vol. 278, no. 1–2, pp. 257–283 (2004).

[19] J. Aboudi and T. O. Williams, "A coupled micro-macromechanical analysis of hygrothermoelastic composites," *Int. J. Solids Struct.,* vol. 37, no. 30, pp. 4149–4179 (2000).

[20] V. V. S. Rao and P. K. Sinha, "Dynamic response of multidirectional composites in hygrothermal environments," *Compos. Struct.,* vol. 64, no. 3–4, pp. 329–338 (2004).

[21] M. H. Zhao, H. Y. Dang, C. Y. Fan, and Z. T. Chen, "Three-dimensional steady-state general solution for isotropic hygrothermoelastic media," *J. of Ther. Stres.*, vol. 41, no. 8, pp. 951-972 (2018).

[22] J. Tong, B. K. Zhang, Z. L. Xu, J. Su, and P. F. Hou, "Two-dimensional steady-state general solutions for isotropic hygrothermoelastic media with applications," *Zeitsc. Fur. Angew. Math. Phys.*, vol. 70, no. 5, pp. 1-15 (2019).

[23] A. Montanaro, "On Singular Surfaces in Isotropic Linear Thermoelasticity with Initial Stress," *J. Acoust. Soc. Am.*, vol. 106, no. 3, pp. 1586–1588 (1999).

[24] M. I. A. Othman and Y. Song, "Reflection of Plane Waves from an Elastic Solid Half-Space Under Hydrostatic Initial Stress Without Energy Dissipation," *Int. J. Solids Struct.*, vol. 44, no. 17, pp. 5651–5664 (2007).

[25] B. Singh, A. Kumar, and J. Singh, "Reflection of Generalized Thermoelastic Waves from a Solid Half-Space Under Hydrostatic Initial Stress," *Appl. Math. Comp.*, vol. 177, no. 1, pp. 170–177 (2006).

[26] B. Singh, "Effect of Hydrostatic Initial Stress on Waves in a Thermoelastic Solid Half-Space," *Appl. Math. Comp.*, vol. 198, no. 2, pp. 494–505 (2008).

[27] B. Singh, "Wave Propagation in an Initially Stressed Transversely Isotropic Thermoelastic Solid Half Space," *Appl. Math. Comp.*, vol. 217, no. 2, pp. 705–715 (2010).

[28] S. M. Abo-Dahab, "Reflection of P and SV Waves from a stress-free Surface Thermoelastic Half-Space Under the Influence of a Magnetic Field and Hydrostatic Initial Stress Without Energy Dissipation," *J. Vib. Control*, vol. 17, no. 14, pp. 2212–2221 (2011).

[29] I. A. Abbas and M. I. Othman, "Generalized Thermoelastic Interaction in a Fibre-Reinforced Anisotropic Half Space Under Hydrostatic Initial Stress," *J. Vib. Control*, vol. 18, no. 2, pp. 175–182 (2012).

[30] M. I. Othman and S. Y. Atwa, "Thermoelastic Plane Waves for an Elastic Solid Half-Space Under Hydrostatic Initial Stress of Type III," *Meccanica*, vol. 47, no. 6, pp. 1337–1347 (2012).

[31] A. K. Yadav, H. S. Mahato, S. Kumari, and P. Jurczak, "Analysis of reflection of wave propagation in magneto-thermoelastic nonlocal micropolar orthotropic medium at impedance boundary," *Int. J. of Nume. Methods for Heat & Fluid Flow*, vol. 34, no. 9, pp. 3416–3437 (2024).

[32] S. Kapila, H. Nagar, and S. Sharma, "MSM fractional calculus operator pertaining to generalized modified Bessel function of the second type," *J. of Inter. Mathe.*, vol. 27, no. 8, pp. 1749–1755 (2024).

[33] W. J. Chang and C. I. Weng, "An analytical solution to coupled heat and moisture diffusion transfer in porous materials," *Int. J. of Heat and Mass Trans.,* vol. 43, no. 19, pp. 3621-3632 (2000).

[34] Y. C. Yang, S. S. Chu, H. L. Lee, and S. L. Lin, "Hybrid numerical method applied to transient hygrothermal analysis in an annular cylinder," *Int. Commu. in Heat and Mass Trans.,* vol. 33, no. 1, pp. 102-111 (2006).

[35] P. Ailawalia, D. Gupta, and V. Sharma, "Surface waves in hygrothermoelastic half-space with hydrostatic initial stress," *Mecha. of Adv. Mate. and Struc.,* vol. 29, no. 16, pp. 2380–2389 (2022).

[36] M. H. Zhao, H. Y. Dang, C. Y. Fan, and Z. T. Chen, "Three-dimensional steady-state general solution for isotropic hygrothermoelastic media," *J. of Ther. Stres.*, vol. 41, no. 8, pp. 951-972 (2018).

[37] S. Kumar, H. Nagar, and S. Kumari, "Reflection of Plane Wave at the Interface Between Thermoelastic and Hygrothermoelastic Solid Half Space," *Mech. Solids*, vol. 60, pp. 384–402 (2025).

[38] P. Ailawalia, A. Sharma, A. M. S. Mahdy, and E. S. Elidy, "Analysis of a non-Homogeneous Hygro-Thermoelastic Layer Immersed in Non-Viscous Fluid," *Mech. Solids,* vol. 60, pp. 1387–1403 (2025).

[39] S. Kumari, Bharti, and B. Singh, "Effects of Two-Temperature on Rayleigh Wave in Generalized Magneto-Thermoelastic Media with Hydrostatic Initial Stress," *J. Heat Trans.*, vol. 141, no. 7, pp.1-7 (2019).

[40] H. Sharma and S. Kumari, "Effects of Two-Temperature, Rotation, Initial Stressed Magnetic Field on Rayleigh Wave in Half-Plane," *J. Heat Trans.,* vol. 142, no. 4, pp. 1-7 (2020).

[41] S. Kumar, H. Nagar, and S. Kumari, "Plane wave reflection in micropolar hygro-thermoelastic half-space," *J. of Ther. Stres.,* vol. 47, no. 1, pp. 1–19 (2024).

Received October, 2025